JOURNAL OF SOLID STATE CHEMISTRY 40, 189–196 (1981)

# The Kinetics of Oxidation of $\phi$-Phase Terbium Oxide: $\frac{7}{2}Tb_2O_{3+\delta} + (\frac{3}{4} - \frac{7}{4}\delta)O_2 \rightarrow Tb_7O_{12}$

TADASHI SUGIHARA,* SHENG H. LIN, AND LEROY EYRING†

*Department of Chemistry and Center for Solid State Science, Arizona State University, Tempe, Arizona 85281*

Received May 22, 1981; in final form July 13, 1981

Kinetic and thermodynamic studies of the terbium oxides between the $Tb_2O_{3+\delta}$ ($n = 4$) and $Tb_7O_{12}$ ($n = 7$) phases of the homolgous series, $Tb_nO_{2n-2}$, have been carried out as a function of oxygen pressure at 708, 740, 772, and 806°C. The thermodynamic study shows a reproducible hysteresis loop which depends on the temperature and pressure. The kinetic study was carried out by measuring the weight gain of an oxide sample in an oxygen atmosphere as a function of time. The results are interpreted by a mixed-model mechanism of diffusion and phase boundary reaction control. The relative fit of the data with other models, including the phenomenological model previously found satisfactory for a related reaction, is shown. The kinetics in the final stage are strongly affected by the existence of pseudophase behavior near $Tb_7O_{12}$. From measurement of the oxygen pressure and temperature dependence of the observed rate constants, the activation energies for the diffusion process and phase boundary reaction process were determined to be −14 and 10 kcal/mole, respectively.

## Introduction

The terbium oxides belong to a fluorite-related homologous series ($R_nO_{2n-2}$, $n = 4$, 7, $10\frac{1}{3}$, 11, 12, $\infty$) of intermediate phases with well-defined stoichiometries and ordered phases (*1*, *2*). Thermodynamic studies of cyclic phase reactions between these intermediate phases reveal reproducible hysteresis loops (*3–5*). Chemical hysteresis, the irreversible reaction cycle between two phases, is far from understood in spite of its prevalence in many oxide systems.

Recently, a thermodynamic model of hysteresis based on the regular solution theory was developed invoking metastabilities (*6*). However, the model can only provide the gross features of the hysteresis loop between two phases. Although there are a variety of causes of hysteresis, the key to understanding the nature and mechanism of chemical hysteresis lies in the detailed knowledge of the structural and thermodynamic relationships of the end-numbers of the phase reaction and of their intergrowth kinetics.

Kinetic and thermodynamic studies of the phase reaction between the $\iota$ phase ($Pr_7O_{12}$) and $\zeta$ phase ($Pr_9O_{16}$) have been reported (*7*). These two phases in the praseodymium oxide system have a well-defined and simple structural relationship

* On leave from the Department of Chemistry, Faculty of Science, Tokyo Institute of Technology, Tokyo, Japan.

† Author to whom inquiries should be addressed.



0022-4596/81/140189-08$02.00/0

(*8*). The kinetic results were interpreted by a phenomenological treatment of the phase reaction data. An analogous model has been used to interpret the phase reaction between $Pr_7O_{12}$ and the $\alpha$ phase ($PrO_{2-x}$) (*9*). This model, using information from the hysteresis loop, has revealed the role of the oxidation path of the hysteresis loop in the phase oxidation.

## Experiments

Kinetic and thermodynamic measurements of the phase oxidation reaction

$$\tfrac{7}{2}Tb_2O_{3+\delta}(s) + (\tfrac{3}{4} - \tfrac{7}{4}\delta)O_2(g) \rightarrow Tb_7O_{12}(s)$$

have been carried out on single-crystal specimens. The single crystals were grown by the hydrothermal method (*10*) and sieved to select crystals in the range 0.01–0.05 mm diameter.

The thermodynamic and kinetic runs were made thermogravimetrically on a Cahn 1000 electrobalance. About 0.51 g of $TbO_{1.95}$ crystals were placed in a platinum bucket 5 mm in height and 15 mm diameter in a uniform temperature zone of a controlled furnace. The experimental error in the weight measurement due to irreproducibility for each run and the thermomolecular flow corrections was estimated to be ±0.02 mg, corresponding to a compositional uncertainty of ±0.0005 in oxygen/metal ratio.

The detailed experimental procedures have been described previously (*7*). In the kinetic runs the samples were kept in a reduced pressure for more than 2 days at higher temperatures (4 days at lower temperatures) to insure the complete reduction to C-type $Tb_2O_3$, $\phi$ phase, and reproducible kinetic data. The final readings of each run were taken 4–12 hr later when the reaction was completed. In the hysteresis study, it took a rather short time (ca. 30 min) to achieve equilibrium in the nonstoichiometric single-phase regions of $\phi$ and $\iota$ phases, but a long time (from 15 to 50 hr) in the hysteresis regions. Since the $\phi$ phase shows a significant compositional variation within our experimental range (see Fig. 1), care was taken to have almost the same composition at the start of each cycle; however, the kinetics are scarcely affected by the variation of composition of the $\phi$ phase.

## Results

### *The Thermodynamic (Hysteresis) Study*

An isothermal hysteresis study was carried out between $\phi$ and $\iota$ phases at different temperatures by changing the pressure. The results are shown in Fig. 1. The compositions of the terbium oxides were not determined absolutely, rather the O/Tb ratio of the iota phase at each temperature was set as 1.714 on the basis of previous experience. (*2*).

The complete loop shifts to higher pressures and increases in width as the temperature increases. The loops are not symmetrical in this case, as are those of the $\iota \rightarrow \zeta$ reaction in the praseodymium oxides (*7*), rather, the oxidation branches are markedly curved. The features of the hysteresis curves are analogous to those obtained in isobaric studies (*3*, *4*). Four distinct regions (*11*) (i.e., $\phi$ phase, $\phi + \iota$ pseudophase, $\iota$

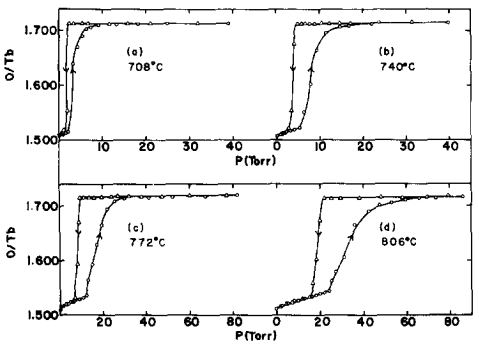


FIG. 1. Isothermal hysteresis loops between $\phi$ and $\iota$ phases at 708, 740, 772, and 806°C.

pseudophase, and ι phase) are clearly shown along the oxidation path.

*The Kinetic Study*

The results of a kinetic run at 806°C and a final pressure of 74.3 Torr are listed in Table I and shown in Fig. 2 as a typical example. The weight fraction, $f$, of the product is plotted against time and compared in this figure to three theoretical models of solid-state reaction which have well-defined and frequently observed mechanisms. The calculated curve is chosen to fit the experimental plot at $f = 0.7$. Agreement between theory and experiment is unsatisfactory.

It is noted that the experimental curve does not approach $f = 1$ as quickly as do the theoretical models in the final stage. In fact, the reaction is completed after about 2 hr, whereas all of the theoretical models go to $f = 1$ within 300 sec.

TABLE I

THE OXIDATION OF $Tb_2O_{3+\delta}$ TO $Tb_7O_{12}$ AT 806°C AND 74.3 Torr OXYGEN

| Time (sec) | $f$ | Time (sec) | $f$ |
|---|---|---|---|
| 2.5 | 0.18[a] | 60.0 | 0.829 |
| 5.0 | 0.242 | 65.0 | 0.850 |
| 7.5 | 0.312 | 70.0 | 0.869 |
| 10.0 | 0.366 | 75.0 | 0.883 |
| 12.5 | 0.411 | 80.0 | 0.896 |
| 15.0 | 0.450 | 85.0 | 0.907 |
| 32.5 | 0.485 | 90.0 | 0.916 |
| 20.0 | 0.516 | 95.0 | 0.923 |
| 22.5 | 0.546 | 100.0 | 0.929 |
| 25.0 | 0.575 | 105.0 | 0.934 |
| 27.5 | 0.602 | 110.0 | 0.939 |
| 30.0 | 0.627 | 115.0 | 0.943 |
| 32.5 | 0.651 | 120.0 | 0.946 |
| 35.0 | 0.673 | 125.0 | 0.947 |
| 37.5 | 0.694 | 130.0 | 0.950 |
| 40.0 | 0.712 | 135.0 | 0.952 |
| 42.5 | 0.731 | 140.0 | 0.955 |
| 45.0 | 0.747 | 145.0 | 0.956 |
| 47.5 | 0.764 | 150.0 | 0.956 |
| 50.0 | 0.778 | 175.0 | 0.964 |
| 55.0 | 0.805 | 200.0 | 0.965 |

[a] The reading was affected by the motion of oxygen introduced into the reaction chamber to initiate the reaction.

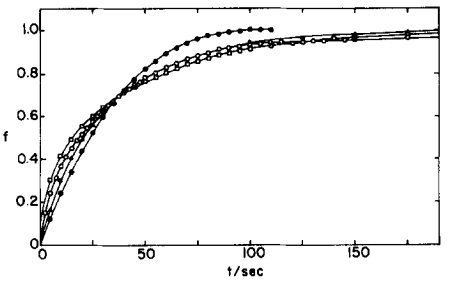


FIG. 2. A typical kinetic run at 806°C and a final pressure of 74.3 Torr. The fraction of reaction ($f$) is plotted against time as indicated, for the original data (open circles) and for three models. The diffusion model, the phase boundary control, and the phenomenological model are marked with squares, closed circles, and triangles, respectively.

The reaction rate $U_{0.7}$, which is defined as the inverse of $t_{0.7}$ (the time required for 70% reaction), plotted against pressure shows a linear relationship as shown in Fig. 3. The pressures determined by extrapolation of these lines to zero rate are strongly dependent upon the temperature and are between the initial and final pressures of the oxidation branch of the hysteresis loop.

## Discussion

In the experimental measurements described above, only information about the

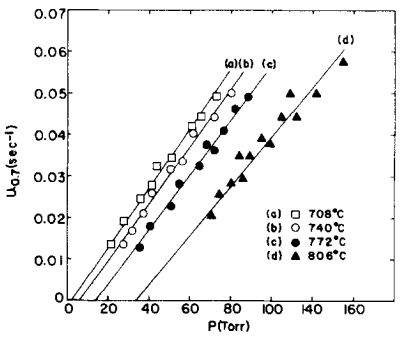


FIG. 3. $U_{0.7}$, the reciprocal of the time required for 70% reaction, against pressure at 708, 740, 772, and 806°C.

weight change of the sample as a function of time at a particular temperature and pressure is obtained. Thus, in order to find rate constants which reflect the elementary processes associated with the phase reaction of terbium oxide, the experimental kinetic data must be fitted to a particular mechanistic model. Many different models for solid-state reactions have been solved and compiled (*12–15*). In this study, several plausible models were tried in fitting the experimental data including simple diffusion, phase boundary reaction control, nucleation and growth, and the phenomenological model.

Since the initial stage of a solid-state reaction involves nucleation and growth (*16*, *17*) this model (*18*, *19*) is considered first. The Avrami equation is probably the best formulation for the kinetics of nucleation and growth.

$$-\ln(1-f) = A\left[e^{-kt} - 1 + kt - \frac{(kt)^2}{2} + \frac{(kt)^3}{6}\right]. \quad (1)$$

The formulation is complex and has only been evaluated in the following special cases:

(i) For $kt \ll 1$,

$$f \simeq kt^4 \quad (2)$$

and

(ii) for $kt \gg 1$ (that is, the reaction is fairly advanced and has already progressed for a certain time) Eq. (1) reduces to

$$f = 1 - e^{\text{const}\cdot t^3}. \quad (3)$$

Both these limiting cases give the general Erofeev Equation,

$$-\ln(1 - f) = (kt)^n. \quad (4)$$

This model cannot explain our experimental results since $df/dt$ would equal 0 at $t = 0$ (Eq. 2), while the data show that $df/dt$ is finite at $t = 0$. Furthermore, our experimental curve does not have the sigmoidal shape required by the Avrami equation.

A plot of log $[-\ln(1 - f)]$ against log $t$ allows the evaluation of $n$ in Eq. (4). The integral power, $n$, has obvious physical significance. When $n = 1$, first-order kinetics is obeyed (*15*). This may signify small-particle nucleation and growth (*17*) or perhaps grain boundary nucleation (*20*). Values of $n = 2$ or 3 suggest that the reaction mechanism involves two- or three-dimensional growth. Figure 4 shows some examples of plots of log $[-\ln(1 - f)]$ vs log $t$ at 708 and 806°C. The plots are linear but $n$ varies from 0.75 to 0.92. This traditional nucleation and growth model based on an initial random nucleation and finally the impingement of the growing nuclei fails to explain our kinetic results.

The induction period required by the Avrami formulation is missing in the oxidation of terbium sesquioxides as is clear from the typical experimental curve shown in Fig. 2. This indicates that the nucleation step occurs virtually instantaneously covering the surface of each reactant particle with a layer of product. This process could lead to a moving boundary controlled mechanism which will be discussed below.

In a previous paper (*7*), a new kinetic equation termed the phenomenological model which depends on the oxidation branch of the hysteresis loop was proposed and the oxidation kinetics of $PrO_{1.714}$ to $PrO_{1.778}$ was thereby explained satisfacto-

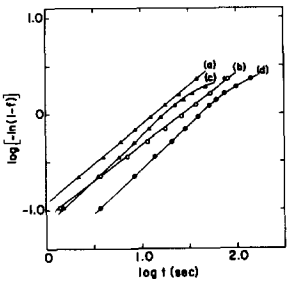


FIG. 4. A test of the fit of the nucleation and growth model, the Avrami equation, at 708 and 806°C. (a) $P$ = 135 Torr; (b) $P$ = 74.4 Torr at 806°C; (c) $P$ = 65.0 Torr; (d) $P$ = 27.3 Torr at 708°C.

rily. The phenomenological equation is expressed as

$$\frac{\beta(1-f)}{\beta-f} = \exp[-k(P-P_n)t], \quad (5)$$

where $\beta = (P - P_0)/(P_n - P_0)$, $P_0$ and $P_n$ indicate the initial and final pressures of the oxidation branch of the hysteresis loop, respectively. The plot of Eq. (5) is compared with the experimental results in Fig. 2 where $P_0 = 24.0$, $P_n = 44.0$ and $\beta = 2.515$ were employed. Agreement between theory and experiment in this case is not good. The phenomenological model equation provides the same result as that obtained from Eq. (4) using $n = 1$ when $\beta > f$. It is clear that the applicability of this model for these phase reactions showing hysteresis loops is limited.

In the case of the simple diffusion model, the fractional weight change, f, for spherical particles (*20*) is given by

$$f = 1 - \frac{6}{\pi^2}\sum_{n=1}^{\infty}\frac{1}{n^2}\exp(-n^2 D^* t), \quad (6)$$

where $D^* = \pi^2 kd/r_0^2$, $r_0$ is the radius of a reactant particle. In Fig. 2 the simple diffusion model is fitted to the curve at $f = 0.7$. The fit is unsatisfactory. The diffusion constant of oxygen in the $\iota$ phase of terbium oxide has not been measured. However, diffusion of oxygen in $Pr_7O_{12}$, which is isomorphous with $Tb_7O_{12}$, has been measured and its diffusion constant ranges around $5 \times 10^{-10}$ cm$^2$/sec whether the form is a powdered or single-crystal specimen (*22*). If we take this to be the diffusion constant of oxygen in the terbium $\iota$ phase and use 0.03 mm as the diameter of the single crystal, $D^*$ is calculated to be $10^{-3}$ sec$^{-1}$. Since this is within an order of magnitude of the reaction rate, $U_{0.7}$, for the single-crystal sample (see Fig. 3), it cannot be ignored. We may expect, therefore, that the diffusion process plays some role in the oxidation kinetics. Although several investigators (*23, 24*) have interpreted their data by Eq. (6), this equation is only applicable to a diffusion process in the absence of chemical reaction. When diffusion occurs toward a sharp boundary where a chemical reaction takes place, the situation becomes entirely different. Furthermore, Eq. (6) cannot explain the linear relationship between $U_{0.7}$ and pressure. Where diffusion into a sphere occurs with reaction, a mathematical model has been developed (*12*). Unfortunately, the equation is so complex that it is difficult to evaluate numerically.

Another plausible model frequently employed to fit experimental kinetic data is that of a moving boundary mechanism. According to this, after nucleation proceeds extremely rapidly on the surface of the crystal, the reaction takes place at the interface between the product and reactant and the thickness of the product layer is changing with time. For a spherically symmetric system, the model has been solved only when the steady state approximation has been used (*12, 13, 25*). In this case, the expression for $f$ is given by

$$Kt = R[1 - (1-f)^{1/3}] + \tfrac{1}{2} - \tfrac{1}{2}(1-f)^{2/3} - f/3, \quad (7)$$

where $R = k_d/(k_p r_0)$, $K = k_d(C^* - C_{eq})/C_0 r_0^2$, $C_0$ represents the concentration of the reactant; C* is the concentration at any time, $t$; $C_{eq}$ is the equilibrium concentration; $k_p$ and $k_d$ are the reaction rate constant and the diffusion constant, respectively. This type of equation has been widely used in kinetic studies. It should be noted that when $f = 1$, $t = (R + \frac{1}{6})/K$. Two limiting cases of Eq. (7) are distinguished.

Case (1): When R is very large, that is $k_p \ll k_d$, or for very small particles, the so-called phase boundary reaction controlled model is obtained with the equation

$$f = 1 - (1 - k't)^3. \quad (8)$$

In this case, $k' = K/R = k_p(C^* - C_{eq})/$

$C_0 r_0$, which depends on $k_p$ alone.

Case (2): If $k_p \gg k_d$ one obtains, by letting $R \to 0$,

$$Kt = \tfrac{1}{2} - \tfrac{1}{2}(1 - f)^{2/3} - f/3. \quad (9)$$

This equation represents a diffusion-controlled mechanism involving $k_d$ alone; therefore, Eq (7) can be called a mixed model.

Theoretical curves are depicted for diffusion (Eq. 6) and for phase boundary control (Eq. 8) with the experimental one in Fig. 2. The curve of Eq. (6) agrees with that of Eq. (9) except in the final stages. Agreement between theory and experiment is not good. However, the experimental curve passes between the two. This suggests that there are two processes, diffusion and phase boundary reaction, in competition which determine the rate of the reaction. Therefore, Eq. (7) should apply to the experimental results.

If we can assume that $C^* = \alpha P$ and $C_{eq} = \alpha P_{eq}$, where $\alpha$ is a proportionality coefficient, then from Eq. (7)

$$U_{0.7} = \frac{1}{t_{0.7}} = \frac{\alpha k_d}{C_0 r_0^2 (0.3306R + 0.04260)} (P - P_{eq}) \quad \text{at } f = 0.7. \quad (10)$$

Equation (10) can explain the linear relationship between $U_{0.7}$ and the pressure as shown in Fig. 3 if $R$ is constant at each temperature. $P_{eq}$ is the minimum $P$ to cause the reaction and might be set equal to the final pressure of an idealized isothermal hysteresis loop. [See Fig. 7 in Ref. (7).]

In order to obtain $R$ values, $U_{0.5}$ (the reciprocal of the time required for 50% reaction) is evaluated as a function of ambient pressure. The plots of $U_{0.5}$ against pressure are similar to those for $U_{0.7}$ vs $P$ shown in Fig. 3. $R$ values can be calculated by comparing the slopes of both $U_{0.7}$ and $U_{0.5}$ and the results are summarized in Table II.

In Fig. 5a–c, the application of Eq. (7)

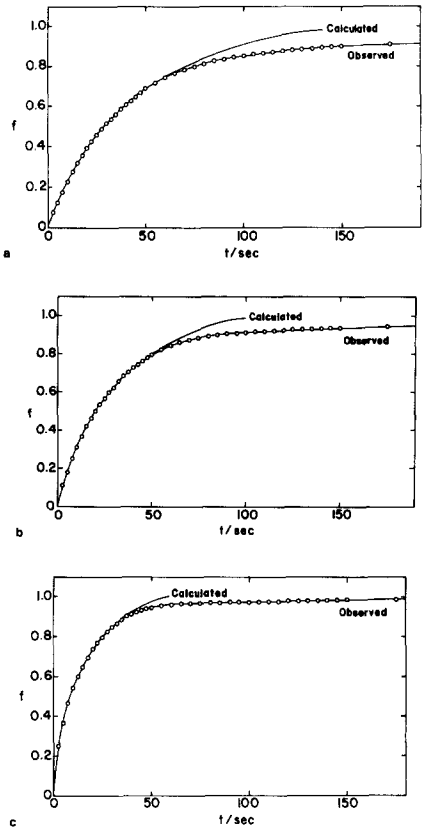


FIG. 5. A test of the fit for a combined diffusion and phase boundary control. (a) 708°C, $P_{O_2}$ = 27.3 Torr; (b) 740°C, $P_{O_2}$ = 41.5 Torr; (c) 806°C, $P_{O_2}$ = 135 Torr.

with the appropriate value of $R$ is used to fit the experimental plot of $f = 0.7$. As can be seen from these figures, the agreement between theory and experiment is satisfactory except for the final stages of the reaction.

The weight fraction, $f$, at which the deviation from experiment begins, depends strongly on the temperature, and ap-

TABLE II

| Temp (°C) | $U_{0.7}$ | $R$ |
|---|---|---|
| 806 | 0.000595 ($P$ − 33.5) | 0.05 |
| 772 | 0.000660 ($P$ − 14.5) | 0.09 |
| 740 | 0.000690 ($P$ − 6.5) | 0.11 |
| 708 | 0.000725 ($P$ − 2.3) | 0.17 |

proaches 1 as the temperature increases (see also Fig. 4). The reaction speed decreases sharply in this region requiring a long time for completion. This indicates that there are at least two different kinds of reactions in the oxidation from $\phi$ to $\iota$.

Four distinct compositional regions occur along the oxidation branch (that is $\phi$, $\phi$ + pseudophase of $\iota$, pseudophase of $\iota$ and $\iota$) as shown in Fig. 1. The same behavior is shown in the calorimetric measurements (*11*). Since the reaction proceeds along the oxidation branch the following sequence should be observed:

$$\underset{(\phi)}{Tb_2O_{3+\delta}} \xrightarrow{\text{step (1)}} \underset{\text{(pseudophase of } \iota)}{Tb_7O_{12-\delta}} \xrightarrow{\text{step (2)}} \underset{(\iota)}{Tb_7O_{12}}.$$

Since the pseudophase of $\iota$ behaves like a single phase (4) and its composition depends on temperature, we can conclude that the mixed model describes reaction step (1), while another mechanism governs the reaction in step (2). Oxygen diffusion through the $\iota$ phase does not seem to be rate controlling in step (2) because it is relatively fast (see the theoretical curve for diffusion in Fig. 2).

From the slopes of the straight lines in Fig. 3, we can determine $\alpha k_d/C_0 r_0^2$ as a function of temperature using appropriate $R$ values. If $\alpha/C_0 r_0^2$ is considered to be the same for all temperatures, an Arrhenius plot of ln $(\alpha k_d/C_0 r_0^2)$ vs $1/T$, as shown in Fig. 6, yields an activation energy ($E_d$) of $-14$ kcal/mole for the diffusion process. Since oxygen diffusion in the terbium oxide has seemed to take place via oxygen vacancies and/or interstitials, the observed diffusion constant can be written as

$$k_d = k_d^0[O], \tag{11}$$

where $k_d^0$ is a vacancy (or interstitial) diffusion coefficient and [O] is a vacancy (or interstitial) concentration of oxygen. We have no knowledge of the concentration, which depends on ambient oxygen pressure and temperature. In fact, the diffusion constant of the $\iota$ phase in the praseodymium oxide system shows a complex oxygen pressure dependence, and Lau *et al.* (*22*) have proposed the following expression to explain the observed results:

$$k_d = a_1 P_{O_2}^{1/2} + a_2 P_{O_2}^{1/6} + a_3 P_{O_2}^{-1/6} + a_4 P_{O_2}^{-1/2}. \tag{12}$$

We suggest that the vacancy (or interstitial) concentration of oxygen decreases as temperature increases as it does in the case of magnetite (*26*, *27*) to account for the negative activation energy of the diffusion process. Furthermore, from the definition of $R$ and the Arrhenius equation

$$R = \frac{k_d}{k_p r_0} = \frac{k_d'}{k_p' r_0} \exp\{-(E_d - E_p)/RT\}, \tag{13}$$

where $k_d'$, $k_p'$ are preexponential factors

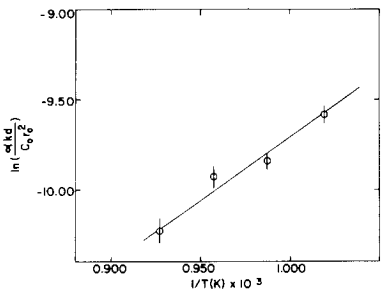


FIG. 6. A function of the rate constant for the combined reaction is plotted against the reciprocal of the absolute temperature.

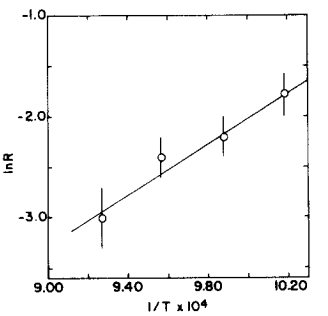


FIG. 7. An Arrhenius plot of rate constant ratio.

and $E_d$, $E_p$ are activation energies, respectively. Arrhenius plots of $R$ are shown in Fig. 7. An activation energy ($E_p$) of 10 kcal/mole is obtained for the phase boundary reaction process.

## Conclusion

At the beginning of the oxidation from $\phi$ phase ($Tb_2O_{3+\delta}$) to $\iota$ phase ($Tb_7O_{12}$), nucleation proceeds extremely rapidly on the surface of the crystal and the surface is covered instantly by a product layer. The reaction rate is then governed by the progress of the resulting interface toward the center of the crystal which is controlled by both diffusion and a phase boundary reaction.

The conversion speed of the transition to the well-ordered $\iota$ phase from the pseudophase of $\iota$, determines the reaction rate in the final stages of the reaction.

## Acknowledgment

We express appreciation to Hideaki Inaba for consultation in the early stages of this study and to Michael Mc Kelvy for the preparation of the single-crystal material from which the specimens were separated. We are also grateful to The National Science Foundation for providing the necessary funds for conducting the research through Grant DMR 78-05722.

## References

1. E. D. Guth and L. Eyring, *J. Amer. Chem. Soc.* **76,** 5242 (1954).
2. B. G. Hyde and L. Eyring, "Rare Earth Research III" (L. Eyring, Ed.), p. 623. Gordon & Breach, New York (1965).
3. J. Kordis and L. Eyring, *J. Phys. Chem.* **72,** 2044 (1968).
4. A. T. Lowe and L. Eyring, *J. Solid State Chem.* **14,** 383 (1975).
5. A. T. Lowe, K. H. Lau, and L. Eyring, *J. Solid State Chem.* **15,** 9 (1975).
6. D. R. Knittel, S. P. Pack, S. H. Lin, and L. Eyring, *J. Chem. Phys.* **67,** 134 (1977).
7. H. Inaba, S. P. Pack, S. H. Lin, and L. Eyring, *J. Solid State Chem.* **33,** 295 (1980).
8. P. Kunzmann and L. Eyring, *J. Solid State Chem.* **14,** 229 (1975).
9. H. Inaba, S. H. Lin, and L. Eyring, *J. Solid State Chem.* **37,** 58 (1981).
10. J. Haschke and L. Eyring, *Inorg. Chem.* **10,** 2267 (1971).
11. H. Inaba, A. Navrotsky, and L. Eyring, *J. Solid State Chem.* **37,** 77 (1981).
12. H. Eyring, S. H. Lin, and S. M. Lin, "Basic Chemical Kinetics." Wiley, New York (1980).
13. J. Szekely, J. W. Evans, and H. Y. Sohn, "Gas–Solid Reactions." Academic Press, New York (1976).
14. G. Pannetier and P. Souchay, "Chemical Kinetics" (H. D. Gesser and H. H. Emond, Trans.). Elsevier, Amsterdam (1967).
15. C. J. Keattch and D. Dollimore, "An Introduction to Thermogravimetry." Hayden, New York (1975).
16. D. A. Young, "Decomposition of Solids." Pergamon, Elmsford, N.Y. (1966).
17. P. W. M. Jacobs and F. C. Tompkins, "Chemistry of the Solid State" (W. E. Garner, Ed.), Chap. 7. Butterworths, London (1955).
18. F. C. Tompkins, "Treatise on Solid State Chemistry" (N. B. Hannay, Ed.), Vol. 4, Chap. 4 Plenum, New York (1976).
19. A. R. Allnatt and P. W. M. Jacobs, *Can. J. Chem.* **46,** 111 (1968).
20. J. Crank, "The Mathematics of Diffusion." Oxford Univ. Press, London/New York (1956).
21. J. W. Cahn, *Acta Metal.* **4,** 449 (1956).
22. K. H. Lau, D. L. Fox, S. H. Lin, and L. Eyring, *High Temp. Sci.* **8,** 129 (1976).
23. D. E. Y. Walker, *J. Appl. Chem.* **15,** 128 (1965).
24. J. Hlavac, *in* "Proceedings, 4th Int. Symp. Reactivity of Solids" (J. H. DeBoer, Ed.), p. 129. Elsevier, Amsterdam (1961).
25. B. B. L. Seth and H. V. Ross, *Trans. Met. Soc. AIME* **233,** 180 (1965).
26. R. Dieckmann and H. Schmalzried, *Ber. Bunsenges. Phys. Chem.* **81,** 344 (1977).
27. R. Dieckmann and H. Schmalzried, *Ber. Bunsenges. Phys. Chem.* **81,** 414 (1977).